

almost no magnetic signal. To study the time evolution (dynamics) of the antiferromagnetic to ferromagnetic transition, the attention is focused on the place marked as “A” on the 3D topography and the MFM image. At time  $t=0$  (i.e. the first measurement performed after bringing back the sample to room temperature), the place marked “A” on the topography (T0) has a height of about 40 nm and is the largest defect site on the surface. This defect site acts as a nucleation centre for the first nucleus of the ferromagnetic phase. The images (T1) and (M1) were obtained after 1 hour. As can be clearly seen, the magnetic signal (ferromagnetic state) at location “A” has increased to slightly more than  $4^\circ$ . The antiferromagnetic to ferromagnetic transition is also coupled to a structural distortion in which the volume of the unit cell in the ferromagnetic phase is slightly larger. Correspondingly, the height of the location “A” has also increased to slightly more than 50 nm [see (T1) in Fig.A.3.1].

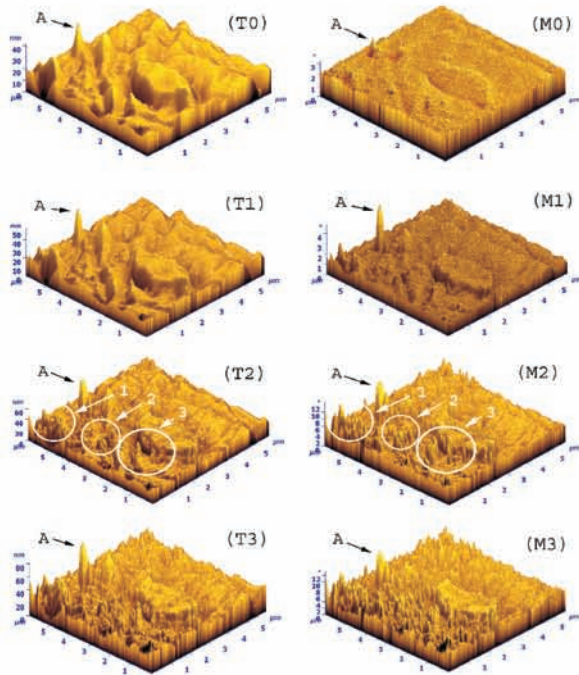


Fig. A.3.1: Time evolution of topography (T0, T1, T2 and T3) and the corresponding magnetic information (M0, M1, M2 and M3). Note the change in scale of the MFM images between M1 and M2, indicating the rise in magnetic signal.

The topography (T2) and MFM (M2) were again recorded after another 1 hour ( $t=2$  hrs). New blisters appear on the topography and the MFM image. These regions are marked as 1, 2 and 3. At  $t=2$  hrs, the height of the location “A” has also increased to almost 70 nm with a corresponding increase in the magnetic signal at the same location. This observation shows that not only the growth of individual

nucleus but also the formation of newer nuclei is governed by intricate coupling between the surface topography and the magnetic structure. Eventually after 3 hours, almost entire sample surface gets crowded with these nuclei of the product ferromagnetic phase ((T3) and (M3)). These results can be interpreted in terms of an intricate coupling between the electronic and elastic degrees of freedom.

In conclusion, direct imaging of the time evolution of initial stages of a first order magneto-structural transition occurring in Fe-Rh alloy has been done. Coexistence of antiferromagnetic and ferromagnetic phase in the sub-micrometer scale is observed. This phase-coexistence, which can be manipulated by applying an external magnetic field or stress, plays a crucial role in the functional properties like, giant magnetocaloric effect, giant elastocaloric effect, giant magnetostriction and giant magnetoresistance of this material. [ See for details : M. Manekar, C. Mukherjee and S. B. Roy *Europhysics Letters*, 80, 17004 (2007).]

Contributed by :

M. A. Manekar (megh @ cat.ernet.in) and C. Mukherjee

## A.4 : Magnetocaloric effect in MnSi

The heating or cooling of a magnetic material because of a variation of applied magnetic field ( $H$ ) is generally referred to as the magnetocaloric effect (MCE). MCE is intrinsic to all magnetic materials. It results from the coupling of a magnetic sublattice with the magnetic field, which changes the magnetic part of the entropy of the material. Materials showing large MCE below 70 K are potential magnetic refrigerants for gas liquefiers. They are also potential “passive” magnetic regenerators for hybrid refrigeration cycles. Recently, we have probed the intermetallic compound MnSi for its MCE characteristics below 70 K. MnSi is an itinerant helimagnet having ordering temperature ( $T_{ord}$ ) just below 30 K. It is known that the application of magnetic field on MnSi at temperatures below  $T_{ord}$  leads to successive field induced phase transitions starting from the zero and low field helimagnetic state to a state with conical spin structure, and then to a high field ferromagnetic state. The temperature gradient of magnetization ( $M$ ) is expected to be large across a magnetic phase transition. The change of magnetic entropy due to applied field is directly related to this temperature gradient of magnetization. Thus MCE is likely to be large near a magnetic phase transition, and this was the motivation to study the MCE in MnSi around  $T_{ord}$  at the Magnetic and Superconducting Materials Section of RRCAT.

The isothermal entropy change ( $\Delta S_M$ ) in MnSi due to an applied magnetic field was estimated from isothermal magnetization ( $M$ ) vs.  $H$  isotherms using the Maxwell's relation:

$$\left(\frac{\partial S_M(T, H)}{\partial H}\right)_T = \left(\frac{\partial M(T, H)}{\partial T}\right)_H$$

Fig.A.4.1.a shows that  $\Delta S_M(T)$  increases with increasing magnetic field. To further understand the effectiveness of MnSi as a potential magnetic refrigerant, the adiabatic temperature change ( $\Delta T_{ad}$ ) in the material because of applied magnetic field was determined.  $\Delta T_{ad}$  was calculated from the temperature dependence of heat capacity ( $C$ ) for MnSi at various constant magnetic fields, using the second law of thermodynamics. Fig.A.4.1.b shows the temperature dependence of  $\Delta T_{ad}$  for MnSi in the presence of various magnetic fields. It is observed that  $\Delta T_{ad}$  is enhanced appreciably with increasing field. It is also observed that  $\Delta T_{ad}$  has a positive sign which signifies that heat is produced in the material when magnetic field is applied. Isothermal entropy change ( $\Delta S_M$ ) due to application of magnetic field was also estimated from  $C(T)_H$  curves, using the expression:

$$\Delta S_M(T)_{\Delta H} = \int_0^T \frac{C(T)_{H_2} - C(T)_{H_1}}{T} dT$$

The change in entropy calculated from isothermal  $M(H)$  and the constant field  $C(T)$  results match with one another. This is clearly seen in Fig.A.4.1.a, and it confirms that  $\Delta T_{ad}$  calculated from the  $C(T)$  results arises solely from the magnetic entropy change due to application of magnetic field.

$\Delta S(T)$  and  $\Delta T_{ad}(T)$  exhibit maxima at temperatures close to  $T_{onb}$ . It is found that  $(\Delta T_{ad})_{max}$  for MnSi is appreciable, and is comparable with the rare-earth intermetallics like  $DyAl_2$ ,  $GdNi_5$ , etc, that are generally considered as large MCE materials in identical fields and similar temperature range. This highlights the importance of MnSi from the point of view of MCE below 70 K. It is observed that the values of  $\Delta S$  and  $\Delta T_{ad}$  for MnSi, obtained for different values of applied fields, are quite large at temperatures well above  $T_{onb}$ , which gives a large working temperature window for a refrigeration cycle having MnSi as the working substance. This is clarified further in the estimation of refrigerant capacity ( $RC$ ) given below.  $RC$  is the heat transferred between the hot and cold reservoirs in one ideal thermodynamic refrigeration cycle. It is defined as:

$$RC = \int_{T_{cold}}^{T_{hot}} [\Delta S(T)]_{\Delta H} dT$$

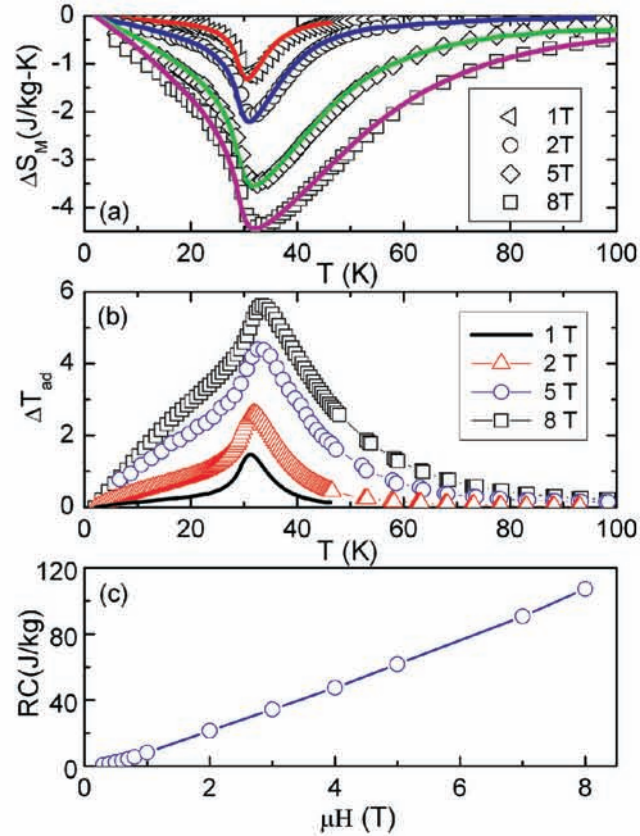


Fig.A.4.1: a) Temperature dependence of the isothermal entropy change ( $\Delta S_M$ ) of MnSi due to applied magnetic field. Open symbols represent  $\Delta S_M$  calculated from magnetization results, while solid lines represent  $\Delta S_M$  obtained from heat capacity results. b)  $T$  dependence of the adiabatic temperature change ( $\Delta T_{ad}$ ) in MnSi due to the applied field. c) Field dependence of the refrigerant capacity.

Fig.A.4.1.c shows the dependence of  $RC$  on the applied magnetic field.  $RC$  of MnSi increases almost linearly with applied magnetic field. It is noted that  $RC$  for MnSi is quite large, and this may be related to the fact that  $\Delta S$  (and  $\Delta T_{ad}$ ) for MnSi are significant over a large temperature regime. Large  $\Delta T_{ad}$  and Refrigerant Capacity, along with low material cost compared to the rare-earth intermetallics make MnSi extremely important as a potential passive magnetic regenerator and as a potential working medium for gas liquefier cycles.

[See for details P. Arora, M.K. Chattopadhyay, and S. B. Roy, *Applied Physics Letters* 91, 62508 (2007)].

Contributed by:  
P. Arora and M.K. Chattopadhyay (maulindu@cat.ernet.in)